

# Numerical Model Investigation for Potential Methane Explosion and Benzene Vapor Intrusion Associated with High-Ethanol Blend Releases

Jie Ma,<sup>†</sup> Hong Luo,<sup>‡</sup> George E. DeVaul,<sup>§</sup> William G. Rixey,<sup>||</sup> and Pedro J. J. Alvarez<sup>†,\*</sup>

<sup>†</sup>Department of Civil and Environmental Engineering, Rice University, 6100 Main Street, Houston, Texas 77005, United States

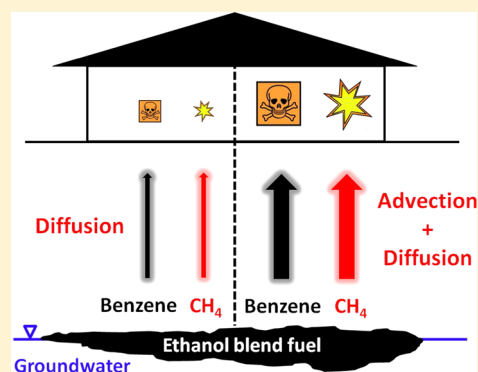
<sup>‡</sup>Chevron Energy Technology Company, 3901 Briarpark Drive, Houston, Texas 77042, United States

<sup>§</sup>Shell Global Solutions (US) Inc., Westhollow Technology Center, 3333 Highway Six South, Houston, Texas 77210, United States

<sup>||</sup>Department of Civil and Environmental Engineering, University of Houston, 4800 Calhoun Rd., Houston, Texas 77204-4003, United States

## Supporting Information

**ABSTRACT:** Ethanol-blended fuel releases usually stimulate methanogenesis in the subsurface, which could pose an explosion risk if methane accumulates in a confined space above the ground where ignitable conditions exist. Ethanol-derived methane may also increase the vapor intrusion potential of toxic fuel hydrocarbons by stimulating the depletion of oxygen by methanotrophs, and thus inhibiting aerobic biodegradation of hydrocarbon vapors. To assess these processes, a three-dimensional numerical vapor intrusion model was used to simulate the degradation, migration, and intrusion pathway of methane and benzene under different site conditions. Simulations show that methane is unlikely to build up to pose an explosion hazard (5% v/v) if diffusion is the only mass transport mechanism through the deeper vadose zone. However, if methanogenic activity near the source zone is sufficiently high to cause advective gas transport, then the methane indoor concentration may exceed the flammable threshold under simulated conditions. During subsurface migration, methane biodegradation could consume soil oxygen that would otherwise be available to support hydrocarbon degradation, and increase the vapor intrusion potential for benzene. Vapor intrusion would also be exacerbated if methanogenic activity results in sufficiently high pressure to cause advective gas transport in the unsaturated zone. Overall, our simulations show that current approaches to manage the vapor intrusion risk for conventional fuel released might need to be modified when dealing with some high ethanol blend fuel (i.e., E20 up to E95) releases.



## INTRODUCTION

Recent U.S. legislation promoting a higher percentage of ethanol in blended fuel will further stimulate the production and consumption of fuel ethanol.<sup>1</sup> Vapor intrusion risk associated with high-ethanol blend releases (E20 up to E95) has been increasingly recognized as a potential concern.<sup>2</sup> Fuel ethanol releases often stimulate methanogenic activity,<sup>3–9</sup> which may pose an explosion hazard when methane accumulates in a confined or poorly ventilated space at 5% to 15% (v/v). Ethanol-derived methane may also increase the vapor intrusion potential of toxic fuel hydrocarbons by stimulating the depletion of oxygen by methanotrophs and thus inhibiting aerobic biodegradation of hydrocarbon vapors.<sup>3,6,10</sup>

Relative high concentrations of methane have been reported in groundwater (23 to 47 mg/L)<sup>3,11,12</sup> and soil gas (15% to 58% v/v)<sup>10,11</sup> that have been impacted by fuel ethanol spills. Although these studies contribute to the understanding of methane generation and migration in the subsurface, none of them directly assessed methane intrusion and accumulation in

overlying buildings. Because of flame quenching within the soil matrix, a methane explosion will not occur in situ in the soil, but may happen when methane accumulates in a confined space above ground where ignitable conditions exist.<sup>5</sup>

Flux chambers have been used to measure methane intrusion and accumulation in confined spaces above fuel ethanol-impacted sites.<sup>3,4</sup> However, flux chamber measurements are not representative of actual vapor flow into buildings, because (1) flux chambers do not have foundations, thus may overestimate the vapor flux into buildings, and (2) flux chambers cannot mimic “building effects” (e.g., depressurization) that play an important role in the vapor subsurface-to-indoor air pathway.<sup>13</sup> Therefore, direct measurements of methane concentrations in the indoor air or model simulations that consider both attenuation across foundations and building effects are

Received: September 3, 2013

Revised: December 10, 2013

Accepted: December 10, 2013

Published: December 10, 2013

necessary to assess the potential explosion risk associated with high ethanol blend releases.

CH<sub>4</sub> gas release by ebullition and advection has previously been noted in a variety of environments, including saturated peat,<sup>14</sup> rice fields,<sup>15</sup> sediment,<sup>16</sup> landfills,<sup>17</sup> and aquifers contaminated by petroleum spills.<sup>18,19</sup> Recent field studies show the importance of CH<sub>4</sub> migration by ebullition and advection at sites impacted by ethanol-blend releases.<sup>4,10</sup> Soil gas advection would enhance the upward migration of methane, thus increasing the potential explosion risk. Another knowledge gap is the impact of biogenic methane on the fate and transport of fuel hydrocarbons in the subsurface. Anaerobic biodegradation processes are relatively slow and do not significantly attenuate hydrocarbon vapor migration through the vadose zone.<sup>20</sup> If sufficient oxygen (e.g., >1%) is present in the unsaturated zone, then biodegradation could reduce hydrocarbon concentrations by several orders of magnitude within a relatively short distance (1–2 m).<sup>21,22</sup> However, the consumption of methane by methanotrophs may deplete available soil oxygen, thus inhibiting aerobic hydrocarbon degradation.<sup>3</sup> These processes are still poorly understood.

With improved understanding of vapor intrusion processes, various mathematical models have been developed to assess potential impacts to indoor air quality.<sup>23–31</sup> Although 1-D analytical models such as the Johnson and Ettinger model<sup>23</sup> are simple, fast, and widely used for screening purposes, 3-D numerical models that consider multispecies transport, reaction, and phase partitioning are more accurate and applicable to describe scenarios with complex model domain and boundary conditions.<sup>25,28,32–35</sup> To our knowledge, such 3-D models have not been used to assess the vapor intrusion risk associated with ethanol-blended fuel releases.

In this study, a 3-D numerical vapor intrusion model<sup>25</sup> was used to simulate various scenarios and quantitatively address: (1) the potential for methane accumulation in buildings overlaying ethanol-blended fuel impacted sites, and the associated explosion hazard; (2) the effect of methane (and associated methanotrophic activity) on the vapor intrusion pathway of benzene; and (3) the impact of gas advection on the vapor intrusion pathway of methane and benzene.

## MATERIALS AND METHODS

**3-D Numerical Model.** The 3-D numerical model used in this study was developed by Abreu and Johnson.<sup>25</sup> This finite difference model solves (1) continuity equations that govern the soil gas pressure distribution and the resulting soil gas velocity field; (2) chemical reactive transport equations that account for diffusion, advection, and biodegradation in the subsurface; (3) air flow and chemical transport through foundation cracks; and (4) chemical mixing with indoor air. The soil characteristics (e.g., porosity, water content, permeability, bulk density, and organic carbon content) can be modeled as homogeneous, layered (up to 10 layers) or heterogeneous. This model also allows for different biodegradation kinetics (nonbiodegradation, zero-order, first-order, Monod) and user-defined building characteristics (e.g., foundation cracks position and size, air exchange rate, and building depressurization). Model outputs include soil gas pressure, soil gas velocity and chemical concentration fields, chemical flux, and indoor air concentration. Details about mathematical model development can be found in Abreu (2005).<sup>36</sup> This model has been used in several studies,<sup>25,32,33</sup> and US EPA guidance on vapor intrusion.<sup>37,38</sup>

## Simulated Scenarios and Model Input Parameters.

This study simulated a symmetrical scenario that includes a single building (10 m × 10 m) located at the center of an open field (48 × 48 m<sup>2</sup>) (Figure 1). The building has a 2 m deep

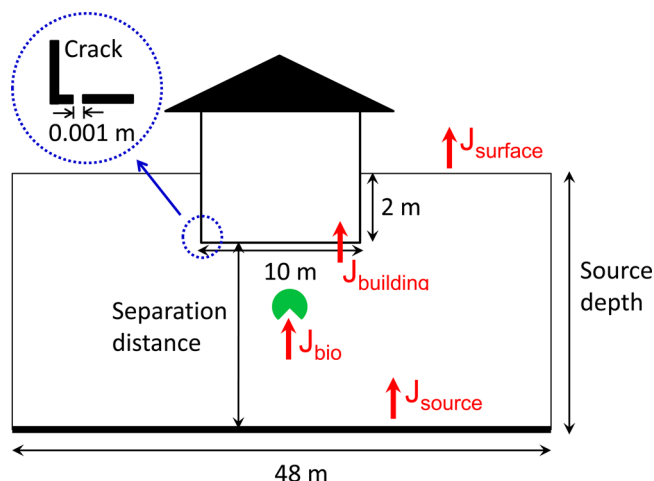


**Figure 1.** Cross-sectional view of the model domain and the perimeter crack on the building foundation (blue dashed circle). The vapor mass fluxes used in following figures includes flux emitted from the source ( $J_{\text{source}}$ ), flux into the building ( $J_{\text{building}}$ ), flux across the soil surface ( $J_{\text{surface}}$ ), and flux biodegraded ( $J_{\text{bio}}$ ).

basement and a perimeter crack (1 mm wide) around the entire foundation of the basement (Figure S1 in the Supporting Information, SI). Similar to other numerical modeling studies,<sup>25,28,32,34–36</sup> the building is assumed to be underpressurized relative to atmosphere by 5 Pa. This pressure difference between building indoor air and atmosphere is generated by a building depressurization effect. The contaminant source zone is located at the bottom of the unsaturated zone and spreads across the entire model domain (48 × 48 m<sup>2</sup>, Figure 1). Four different source depths (3, 5, 8, and 15 m) were chosen. The 3 m depth represents a shallow vapor source case and 15 m depth represents a deep vapor source case. Since the basement has a depth of 2 m, actual separation distance between source zone and building foundation are 1, 3, 6, and 13 m. All simulations were conducted for homogeneous and steady-state scenarios and the associated model input parameters related to CH<sub>4</sub> and benzene source concentrations, source gas pressure, and separation distance are listed in Table 1 (see Figures 1–7). Other model input parameters regarding building and foundation, soil properties, contaminant properties, and biodegradation rate constants were selected based on previous studies (SI Table S1).<sup>25,32,33</sup> These biodegradation rate constants are illustrative of the range of values in the literature, but their use does not imply that these values are universally accepted.

On the basis of the overall stoichiometry of ethanol degradation under fermentative methanogenic conditions (2 CH<sub>3</sub>CH<sub>2</sub>OH = CO<sub>2</sub> + 3CH<sub>4</sub>), the degradation of ethanol could produce gas with up to 75% (v/v) CH<sub>4</sub> content. Therefore, 75 v/v % (4.91 × 10<sup>2</sup> g/m<sup>3</sup>) was chosen as the maximum CH<sub>4</sub> source concentration.

To simulate the CH<sub>4</sub> explosion risk, we considered aerobic CH<sub>4</sub> biodegradation by methanotrophs as it migrates upward through the vadose zone. Since the available oxygen can also be consumed by the biodegradation of other compounds

Table 1. Simulated Scenarios for Table 2 and Figures 1–7 in the Main Text and Tables S2 and S3 and Figures S2–S8 in the SI

	CH <sub>4</sub> source concentration	TPH source concentration	benzene source concentration	source gas pressure	separation distance
Table 2	75%	200 g/m <sup>3</sup>	NA <sup>a</sup>	0 to 200 Pa	3 m
Figure 2	0.015% to 75%	200 g/m <sup>3</sup>	NA	0 Pa	1, 3, 6, and 13 m
Figure 3	0.015% to 75%	200 g/m <sup>3</sup>	NA	0 Pa	6 m
Figure 4	75%	200 g/m <sup>3</sup>	NA	0.1 to 200 Pa	1, 3, 6, and 13 m
Figure 5	0.076% to 75%	NA	0.1 g/m <sup>3</sup>	0 Pa	1, 3, 6, and 13 m
Figure 6	0.015% to 75%	NA	0.1 g/m <sup>3</sup>	0 Pa	6 m
Figure 7	0.015% to 75%	NA	0.1 g/m <sup>3</sup>	0 Pa	6 m
SI Table S2	75%	200 g/m <sup>3</sup>	NA	0 to 200 Pa	1, 6, and 13 m
SI Table S3	75%	200 g/m <sup>3</sup>	NA	0 to 200 Pa	1, 6, and 13 m
SI Figure S2	0.015% to 75%	200 g/m <sup>3</sup>	NA	0 Pa	1 m
SI Figure S3	0.015% to 75%	200 g/m <sup>3</sup>	NA	0 Pa	3 m
SI Figure S4	75%	200 g/m <sup>3</sup>	NA	0 to 200 Pa	3 m
SI Figure S5	0% to 75%	NA	0.1 g/m <sup>3</sup>	0 Pa	6 m
SI Figure S6	0% to 75%	NA	0.1 g/m <sup>3</sup>	0 Pa	6 m
SI Figure S7	0% to 75%	NA	0.1 g/m <sup>3</sup>	0 Pa	6 m
SI Figure S8	75%	NA	0.1 g/m <sup>3</sup>	0.1 to 200 Pa	1, 3, 6, and 13 m

<sup>a</sup>“NA” is the abbreviation for not applicable.

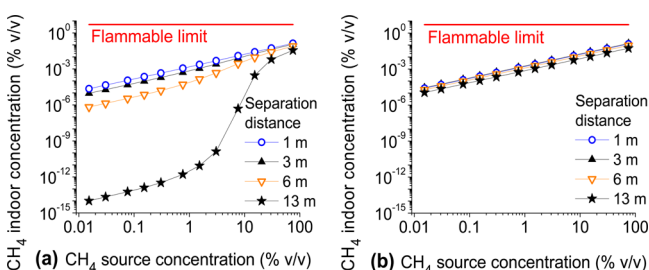


Figure 2. Simulated CH<sub>4</sub> indoor concentrations for different CH<sub>4</sub> source concentrations and separation distances, (a) with and (b) without CH<sub>4</sub> biodegradation. The source was assumed to contain 200 g/m<sup>3</sup> TPH that contribute to the biochemical oxygen demand in the vadose zone. The source pressure is 0 Pa.

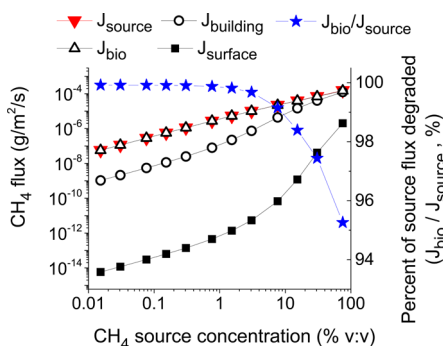


Figure 3. Changes in CH<sub>4</sub> mass flux emitted from the source ( $J_{source}$ ), flux into the building ( $J_{building}$ ), flux across the soil surface ( $J_{surface}$ ), and flux biodegraded ( $J_{bio}$ ) with different CH<sub>4</sub> source concentrations. The right Y-axis shows the percent of source flux degraded ( $J_{bio}/J_{source}$ ). The source also contains 200 g/m<sup>3</sup> TPH that contribute to the biochemical oxygen demand in the vadose zone. The source soil gas pressure is 0 Pa. The separation distance is 6 m.

associated with the release, the model assumes that 200 g/m<sup>3</sup> of the total petroleum hydrocarbons (TPH) were present at the source zone (Table 1). This concentration is representative of nonaqueous phase liquid (NAPL) sources<sup>38,39</sup> and has been used in previous modeling studies.<sup>25,32,36</sup> The properties of these hydrocarbons were assumed to be the same as for benzene vapor (SI Table S1) because model computation slows

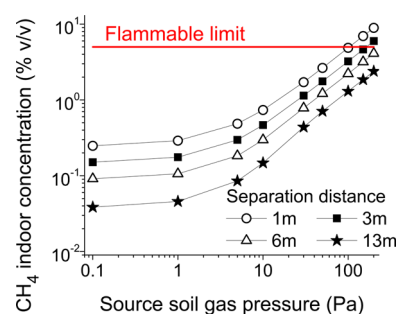


Figure 4. Simulated CH<sub>4</sub> indoor concentrations for different separation distances and source gas pressures. The source contains 75% (v/v) CH<sub>4</sub> and 200 g/m<sup>3</sup> TPH that contribute to the biochemical oxygen demand in the vadose zone. The CH<sub>4</sub> indoor concentration for the source soil gas pressure of 0 Pa can be found in Figure 2a.

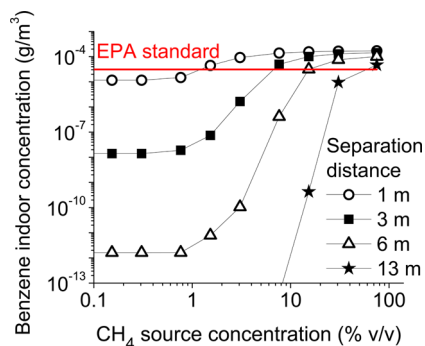
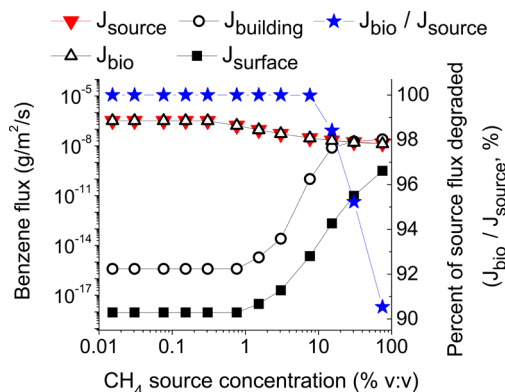


Figure 5. Simulated benzene indoor concentrations for different CH<sub>4</sub> source concentrations and separation distances. The EPA indoor air standard for benzene ( $3.1 \times 10^{-5}$  g/m<sup>3</sup>) corresponds to a  $10^{-4}$  lifetime risk.<sup>48</sup> The source contains 0.1 g/m<sup>3</sup> benzene, with a source soil gas pressure of 0 Pa.

significantly when running multiple fuel constituents. Benzene was not included as a separate component for these simulations because it has a minor effect on the CH<sub>4</sub> mass fluxes.

To simulate the impacts of CH<sub>4</sub> generation on benzene vapor intrusion potential, 0.1 g/m<sup>3</sup> was chosen as the benzene source concentration as a representative value from a petroleum vapor intrusion database.<sup>40</sup> This concentration falls within the



**Figure 6.** Changes in benzene flux emitted from source ( $J_{\text{source}}$ ), flux into the building basement ( $J_{\text{building}}$ ), flux across the soil surface ( $J_{\text{surface}}$ ), and flux biodegraded ( $J_{\text{bio}}$ ) for different  $\text{CH}_4$  source concentrations. The right Y-axis shows the percent of source flux that is biodegraded ( $J_{\text{bio}}/J_{\text{source}}$ ). The source contains  $0.1 \text{ g/m}^3$  benzene, with a source soil gas pressure of 0 Pa. The separation distance is 6 m.

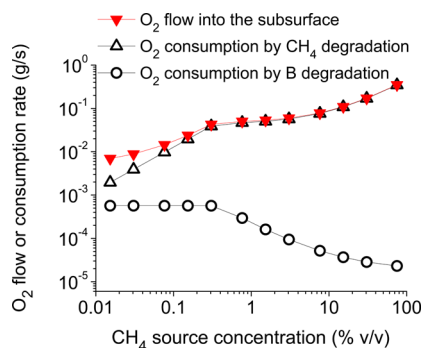


**Figure 7.** Changes in  $\text{O}_2$  consumption by aerobic degradation of benzene (B) and  $\text{CH}_4$  with different  $\text{CH}_4$  source concentrations. The source contains  $0.1 \text{ g/m}^3$  benzene, with a soil gas pressure of 0 Pa. The separation distance is 6 m.

top 25% of benzene vapor concentrations measured near various NAPL sources and compiled. Our intent was to use a benzene concentration representative of commonly reported values rather than the maximum value in site investigations. TPH was not included as a component. This shows the effect that  $\text{CH}_4$  alone has on benzene attenuation. Including  $200 \text{ g/m}^3$  TPH in these cases would directionally, but not significantly, reduce the amount of benzene attenuation. Not including TPH is a more conservative approach for assessing impacts of methane on benzene vapor intrusion.

To simulate the impact of gas advection on migration and intrusion of subsurface  $\text{CH}_4$  and benzene, different source gas pressures (0.1, 1, 5, 10, 50, 100, 150, 200 Pa) were selected (Table 1). Note that the higher simulated pressures may be rare in the high-permeability sandy soils assumed here, but were considered to delineate the potential effects of high-ethanol blend releases under a wide range of conditions. To our knowledge, data on soil gas pressures in the source zone of fuel ethanol releases are not available. However, according to a numerical simulation of soil gas data at a crude oil release site, methanogenesis in the source zone could generate about 1 Pa of source pressure.<sup>18</sup> Landfill sites could have as high as several thousand Pa of source pressure.<sup>41</sup> As a readily degradable compound, the release of large volumes of fuel ethanol usually

stimulates much stronger methanogenic activity than petroleum hydrocarbons, but is unlikely to be stronger than methanogenesis at landfills. Therefore, the source gas pressure at a fuel ethanol impacted aquifer is likely to be higher than that at a petroleum spill site and smaller than that at a landfill site.

#### Assumptions and Limitations of This Modeling Study.

This modeling study has following assumptions: (1) the source zone is nondepleting and infinite; (2) the building is modeled as a perfectly mixed continuously stirred tank reactor (CSTR); (3) no NAPL phase is present in the transport domain (it could be present at the source zone) and chemicals partition among gas, dissolved and adsorbed phases only; and (4) density-driven advective transport is neglected.

Similar to previous studies,<sup>25,32,33</sup> all simulations reported herein assume homogeneous and steady-state conditions. However, real site geologic conditions are usually heterogeneous, complex, and site-specific.<sup>34</sup> Nonsteady state environmental factors such as barometric pressure fluctuations and wind load on buildings could affect the migration and intrusion of gas contaminant into buildings.<sup>42,43</sup> Although a modified version of the Abreu and Johnson model is capable of simulating vapor intrusion during transient wind load and barometric pressure fluctuations,<sup>44</sup> such simulations are time-consuming and require significant computational resources. Therefore, this study simulates quasi-steady scenarios representing short-term average indoor concentrations during periods of net airflow is into the building enclosure. Finally, note that all simulations assumed perimeter cracks, and results may be different for buildings with more centrally located cracks.

Diffusion in this model follows Fick's law, which presumes low concentrations for each soil gas constituent and that their individual fluxes are independent. This is addressed in these model scenarios by specifying, indirectly, through pressures at the model boundaries, a constituent-independent Darcy velocity field for the soil gas. This is a reasonable assumption for the nearly equimolar (and nearly equal volume) aerobic reactions included in the model domain. Also, the effect of displaced, passive nonreactive soil gases (mainly  $\text{N}_2$ ) on flux estimates is not addressed; this would require a different approach, such as a "dusty gas" model.<sup>45,46</sup>

Finally, the model presumes a separating and attenuating layer of vadose-zone soil between the methanogenic source and the building enclosure. Direct entry of methane gas into a building, such as gas evolution through an untrapped or unvented well, sump, or sewer connected to a building, is not evaluated.

## RESULTS AND DISCUSSION

**The Explosion Risk for Diffusion-Driven  $\text{CH}_4$  Migration Is Negligible.** If diffusion is the major mass transport process in the deeper vadose zone (advection may occur in the vicinity of the basement due to building depressurization),  $\text{CH}_4$  is unlikely to build up to the lower flammable level (5% v/v) in overlying buildings.  $\text{CH}_4$  indoor concentrations are simulated for different  $\text{CH}_4$  source concentrations and separation distances, with and without biodegradation (Figure 2). Simulated  $\text{CH}_4$  indoor concentrations increase as source concentrations increase and separation distance decreases. However, even under the worse-case scenario examined here (i.e.,  $\text{CH}_4$  source concentration is 75% v/v, the separation distance is 3 m, and no biodegradation), the simulated  $\text{CH}_4$

Table 2. Simulated Air Flow Rate and CH<sub>4</sub> Flux with Different Source Pressures for a Separation Distance of 3 m<sup>a</sup>

pressure (Pa)	air flow rate (L/min)			CH <sub>4</sub> flux (g-CH <sub>4</sub> /m <sup>2</sup> /s)		
	Q <sub>source</sub>	Q <sub>surface</sub>	Q <sub>building</sub>	J <sub>source</sub> <sup>b</sup>	J <sub>surface</sub> <sup>c</sup>	J <sub>building</sub> <sup>d</sup>
0	0	-0.9 <sup>e</sup>	0.9	2.5 × 10 <sup>-4</sup>	1.2 × 10 <sup>-5</sup>	1.8 × 10 <sup>-4</sup>
0.1	1.1	-0.1	1.2	2.5 × 10 <sup>-4</sup>	1.2 × 10 <sup>-5</sup>	2.4 × 10 <sup>-4</sup>
1	4.5	3	1.3	2.8 × 10 <sup>-4</sup>	1.9 × 10 <sup>-5</sup>	2.8 × 10 <sup>-4</sup>
5	20	18	1.9	4.0 × 10 <sup>-4</sup>	6.9 × 10 <sup>-5</sup>	4.7 × 10 <sup>-4</sup>
10	39	36	3	6.0 × 10 <sup>-4</sup>	1.9 × 10 <sup>-4</sup>	7.4 × 10 <sup>-4</sup>
30	114	109	6	1.6 × 10 <sup>-3</sup>	9.2 × 10 <sup>-4</sup>	1.8 × 10 <sup>-3</sup>
50	190	183	9	2.7 × 10 <sup>-3</sup>	1.8 × 10 <sup>-3</sup>	2.9 × 10 <sup>-3</sup>
100	379	366	16	5.4 × 10 <sup>-3</sup>	4.0 × 10 <sup>-3</sup>	5.3 × 10 <sup>-3</sup>
150	568	549	24	8.1 × 10 <sup>-3</sup>	6.1 × 10 <sup>-3</sup>	7.8 × 10 <sup>-3</sup>
200	757	732	31	1.1 × 10 <sup>-2</sup>	7.9 × 10 <sup>-3</sup>	1.0 × 10 <sup>-2</sup>

<sup>a</sup>The source contains 75% (v/v) CH<sub>4</sub> and 200 g/m<sup>3</sup> TPH. <sup>b</sup>J<sub>source</sub> was calculated by dividing mass flow rate emitted from the source (g-CH<sub>4</sub>/s) by the source area (48 m × 48 m). <sup>c</sup>J<sub>surface</sub> was calculated by dividing mass flow rate across the soil surface (g-CH<sub>4</sub>/s) by the soil surface area (48 m × 48 m - 10 m × 10 m). <sup>d</sup>J<sub>building</sub> was calculated by dividing mass flow rate into buildings (g-CH<sub>4</sub>/s) by the building foundation area (10 m × 10 m). <sup>e</sup>The negative value for Q<sub>surface</sub> means the air flows from atmosphere into the soil due to building depressurization effect.

indoor concentration is still much lower (>20-fold) than the lower flammable level for CH<sub>4</sub> (5% v/v) (Figure 2).

Methanotrophic bacteria could significantly attenuate the mass flux of CH<sub>4</sub> in the unsaturated zone and reduce indoor concentrations and the associated explosion risk (compare Figure 2, parts (a) and (b)). Figure 3 shows the simulated scenarios with a separation distance of 6 m and a TPH concentration of 200 g/m<sup>3</sup>. If the CH<sub>4</sub> source concentration is lower than 1.5% (v/v), then more than 99% of CH<sub>4</sub> flux emitted from the source (J<sub>source</sub>) is degraded before reaching the ground surface, and the percent of source flux that is biodegraded (J<sub>bio</sub>/J<sub>source</sub>) does not change with increasing CH<sub>4</sub> source concentrations (Figure 3). If the CH<sub>4</sub> source concentration is higher than 1.5% (v/v), then the percentage of source flux that is biodegraded (J<sub>bio</sub>/J<sub>source</sub>) decreases as the CH<sub>4</sub> source concentration increases. However, even when the CH<sub>4</sub> source concentration reaches 75% (v/v) and the vapor source is shallow (1 m separation distance), biodegradation still attenuates more than 82% of the upward CH<sub>4</sub> flux (SI Figure S2). Methanotrophic bacteria are widespread in natural environments (they are especially abundant in soil).<sup>47</sup> Our modeling results corroborate previous pilot-scale experimental results<sup>3</sup> and indicate the importance of methanotrophic activity to attenuate CH<sub>4</sub> generated from ethanol plumes and reduce its potential to reach the surface. Note that while the simulated indoor CH<sub>4</sub> concentration does not reach the lower flammable level, the subslab soil gas concentration does (SI Figure S4). This may create other concerns not examined in this study (e.g., CH<sub>4</sub> build up in less ventilated smaller confined spaces).

CH<sub>4</sub> explosion risk in nonpressurized flow can also be assessed using the attenuation factors assembled from the US EPA vapor intrusion database, which contains indoor air measurements of toxic vapors coupled with subslab soil gas, exterior soil gas groundwater, or crawlspace measurements for 913 buildings at 41 sites in 15 U.S. states.<sup>37</sup> By compiling this database, a recent EPA report recommends 0.01 as a conservative subslab attenuation factor (the ratio of indoor air concentration to subslab soil gas concentration, AF<sub>subslab</sub> = C<sub>indoor</sub>/C<sub>subslab</sub>) for chlorinated volatile compounds.<sup>37</sup> Using this attenuation factor and assuming that the source of CH<sub>4</sub> concentration is 75% (v/v), the corresponding CH<sub>4</sub> indoor concentration is only 0.75% (v/v), which is much lower than the lower flammable limit.

### Potential Explosion Risk Increases Significantly for Advection-Driven CH<sub>4</sub> Migration.

A recent field study showed that the accumulation of ethanol-derived methane and carbon dioxide in the source zone could generate a pressure gradient and cause significant advective gas transport in the subsurface.<sup>4</sup> They reported up to 6.3 × 10<sup>-3</sup> g/m<sup>2</sup>/s of surficial CH<sub>4</sub> efflux and 6% to 22% (v/v) of CH<sub>4</sub> concentration in the flux chamber emplaced at a site impacted by the release of a large volume of denatured fuel-grade ethanol.<sup>4</sup> Our simulations corroborate this field study, indicating that if methanogenic activity near the source zone is sufficiently high to cause significant advective gas transport, CH<sub>4</sub> could build up to flammable levels (>5% v/v) in overlying buildings. Scenarios with different source gas pressures (0, 0.1, 1, 5, 10, 30, 50, 100, 150, and 200 Pa) and separation distances (1, 3, 6, and 13 m) were simulated (Figure 4). SI Figure S4 shows that increases in source pressure significantly change the soil gas pressure field distribution, which may change the subsurface air flow and contaminant mass flux. Table 2 lists the simulated air flow rate and CH<sub>4</sub> flux for the separation distance of 3 m. The simulated air flow rate and CH<sub>4</sub> flux for other separation distances are listed in SI Tables S5 and S6, respectively. Simulated CH<sub>4</sub> indoor concentrations for all separation distances are shown in Figure 4. As source gas pressures increase from 0 to 200 Pa, simulated air flow rates from the source (Q<sub>source</sub>) for a separation distance of 3 m increased from 0 to 757 L/min (Table 2), resulting in a 44-fold increase in the CH<sub>4</sub> flux emitted from the source (J<sub>source</sub>) (Table 2). As a result, the simulated CH<sub>4</sub> flux into buildings (J<sub>building</sub>) increases by 56-fold (Table 2), which causes the CH<sub>4</sub> indoor concentrations to increase by more than 60-fold for the separation distance of 3 m (Figure 4). When the separation distance is equal to or less than 3 m and the source gas pressure is higher than 100 Pa, simulated CH<sub>4</sub> indoor concentrations exceed the 5% v/v flammable level, resulting in a potential explosion risk (Figure 4). In this study, we have neglected advective transport due to changes in density. For high CH<sub>4</sub> source concentrations, lower densities relative to air may also contribute to increased upward CH<sub>4</sub> mass fluxes in addition to high source pressures.

To put the simulated CH<sub>4</sub> fluxes data into context, measured CH<sub>4</sub> surficial efflux data in natural and impacted environments are listed in Table 3. The simulated J<sub>surface</sub> for the 75% (v/v) CH<sub>4</sub> source concentration varied by 6 orders of magnitude with different separation distances and source pressures; e.g., 5.1 ×

**Table 3. Measured CH<sub>4</sub> Flux in Natural and Contaminated Environments**

environments	flux (g-CH <sub>4</sub> /m <sup>2</sup> /s)	reference
rice field	$5.7 \times 10^{-7}$ to $1.2 \times 10^{-5}$	50,51
wetlands	$8.0 \times 10^{-8}$ to $4.5 \times 10^{-5}$	52,53
lagoon	$3.1 \times 10^{-9}$ to $6.8 \times 10^{-5}$	54,55
peat	$1.0 \times 10^{-7}$ to $3.6 \times 10^{-5}$	56,57
E95 <sup>a</sup> impacted aquifer	$2.2 \times 10^{-5}$ to $6.3 \times 10^{-3}$	4
landfill	$2.4 \times 10^{-8}$ to $4.6 \times 10^{-2}$	58,59

<sup>a</sup>Ethanol denatured with 5% gasoline.

$10^{-8}$  g/m<sup>2</sup>/s for 0 Pa source pressure and 13 m separation distance to  $1.1 \times 10^{-2}$  g/m<sup>2</sup>/s for 200 Pa source pressure and 1 m separation distance (SI Table S3). Methane mass fluxes lower than  $10^{-3}$  g/m<sup>2</sup>/s are typical for natural methanogenic environments (Table 3). Values greater than  $10^{-3}$  g/m<sup>2</sup>/s have been observed at landfills and sites impacted by ethanol blend fuel releases (Table 3).

**Oxygen Consumption during CH<sub>4</sub> Biodegradation in the Vadose Zone Increases Benzene Vapor Intrusion Potential.** Baseline simulations indicate that if there is no CH<sub>4</sub> generation in the source zone, 0.1 g/m<sup>3</sup> of benzene will not cause a vapor intrusion problem even for a shallow source (e.g., 1 m separation distance). However, CH<sub>4</sub> generation near the source could significantly increase benzene indoor concentrations (Figure 5). As CH<sub>4</sub> source concentrations increase from 0 to 75% (v/v), benzene indoor concentrations increase by 15-,  $1.0 \times 10^4$ -,  $6.2 \times 10^7$ -, and  $6.3 \times 10^{16}$ -fold for separation distances of 1, 3, 6, and 13 m, respectively. Although previous studies indicate a low benzene vapor intrusion potential when the separation distance is larger than 10 m,<sup>32,39,40</sup> our simulations infer that if very high CH<sub>4</sub> concentrations (e.g., 75% v/v) are generated and subsequently consumed in the vadose zone (resulting in O<sub>2</sub> depletion), even a separation distance of 13 m may result in some benzene vapor intrusion and possibly exceed the EPA indoor air screening level of  $3.1 \times 10^{-5}$  g/m<sup>3</sup> that corresponds to a  $10^{-4}$  lifetime risk<sup>48</sup> (Figure 5). Note that US EPA provides target indoor air concentrations for three different lifetime risk levels:  $10^{-4}$ ,  $10^{-5}$ , and  $10^{-6}$ . Our inferences about the significance of benzene vapor intrusion may be different at other risk levels.

Inhibition of benzene biodegradation as methanotrophs consume vadose-zone oxygen is the major reason for the increase in benzene vapor intrusion. Biodegradation attenuates more than 90% of the benzene flux emitted from the source (Figure 6). As CH<sub>4</sub> source concentrations increase from 0.015% (v/v) to 75% (v/v), the benzene flux that is bioattenuated ( $J_{\text{bio}}$ ) decreases 25-fold, and the percent of benzene source flux that is biodegraded ( $J_{\text{bio}}/J_{\text{source}}$ ) decreases from >99.99% to 90.5%. This leads to a significant increase (> $10^7$ -fold) in the benzene flux intrusion into buildings ( $J_{\text{building}}$ ) and transport across the soil surface ( $J_{\text{surface}}$ ), despite a decrease in the benzene flux emitted from the source ( $J_{\text{source}}$ ) by at least 22-fold due to a lower benzene concentration gradient between the source and the slab (Figure 6).

Depletion of O<sub>2</sub> is the major reason for decreases in benzene biodegradation.<sup>49</sup> Under aerobic conditions, CH<sub>4</sub> degrades faster than benzene (see SI Table S1 footnotes). As the CH<sub>4</sub> source concentration increases from 0.015% (v/v) to 75% (v/v), the O<sub>2</sub> consumed by CH<sub>4</sub> degradation increases by 180-fold, thus leading to a rapid decrease (25-fold) in the O<sub>2</sub> that is used for benzene degradation, even though the total O<sub>2</sub> flux entering

into the system increases by more than 50-fold due to a lower O<sub>2</sub> concentration gradient between the soil surface and the vapor source (Figure 7). To better illustrate these processes, changes in the concentration distribution of benzene, CH<sub>4</sub>, and O<sub>2</sub> with different CH<sub>4</sub> source concentrations for a separation distance of 6 m are shown in SI Figures S5, S6, and S7.

Benzene vapor intrusion could be exacerbated if methanogenic activity is sufficiently high to cause significant advective gas transport. Benzene indoor concentrations were simulated for different source gas pressures (SI Figure S8). As the source gas pressure increases from 0.1 to 200 Pa, the advective gas transport strips more benzene from the source zone and thus increases benzene indoor concentrations by at least 40-fold for all four separation distances (SI Figure S8).

**Implications for Site Assessment and Remedial Action.** Guidance for assessing health risks associated with vapor intrusion of petroleum hydrocarbon<sup>39</sup> and chlorinated solvents<sup>37</sup> is relatively well established, but guidance for assessing explosion risks associated with methane vapor intrusion from ethanol fuels is limited. Using a 3-D numerical model, this study indicates that methane is unlikely to reach flammable levels in overlying buildings if diffusion is the major mass transfer process in the deeper vadose zone. However, our simulations show that if methanogenic activity is sufficiently strong (as might occur for releases with high ethanol content) to increase gas pressure and cause advective gas transport near the source zone, CH<sub>4</sub> could build up to potentially flammable levels (>5% v/v) in overlying buildings.

The U.S. EPA's guidance document for petroleum vapor intrusion is based on field measurement data at retail service station sites,<sup>39</sup> including sites for which E10 (10% ethanol fuel) would have been used for decades. According to this document, regular gasoline or E10 releases are unlikely to cause a flammability hazard, unless the gasoline is in the building or in direct contact with the foundation. Therefore, the inferences of our simulations are mainly applicable to releases of high-ethanol content fuels, including E20 up to E95.

Conceptual models of vapor intrusion usually assume that diffusion is the major vapor transport mechanism in the deeper vadose zone, and that advection plays an important role only in the vicinity of the building basement (due to building depressurization). This study indicates that advective soil gas transport generated from the accumulation of fermentative biogas could play an important role in the subsurface vapor transport. Therefore, gas advection should be considered for fuel ethanol impacted sites or other sites where strong fermentation activities exist. Conditions that are conducive to advective gas migration through the vadose zone include (1) high soil moisture content that inhibits diffusion, (2) a shallow source zone, (3) a soil surface that is paved or covered by a large building foundation that inhibits O<sub>2</sub> inflow, (4) release of high ethanol blends (e.g., E85), and (5) a large volume release where the source is not removed.

The U.S. EPA is trying to establish vertical separation criteria for screening vapor intrusion risk at petroleum release sites. Using available field measurement data, recent EPA guidance indicates that 5.5 to 6.1 m of separation distance could reduce soil benzene concentration below a defined soil gas threshold ( $100 \mu\text{g}/\text{m}^3$ ) at 95% of sites that have an NAPL source present.<sup>39</sup> Although that document is based on comprehensive site data, our modeling results indicate that under our simulated conditions, the presence of high concentrations of CH<sub>4</sub> originating from releases of high ethanol blends may deplete

the available soil O<sub>2</sub> and inhibit benzene aerobic degradation, thus resulting in a higher benzene vapor intrusion potential than suggested in the current EPA guidance for gasoline fuel release sites. If methanogenic activity is sufficiently high to generate advective gas transport, then the benzene intrusion rate would be even higher. Therefore, the proposed EPA separation distance criteria for conventional gasoline releases may not apply to higher ethanol content fuels such as E85 and E95.

## ■ ASSOCIATED CONTENT

### ● Supporting Information

Details on model input parameters; simulated air flow rates; and CH<sub>4</sub> flux with different source pressures for different separation distances, changes in pressure field distribution, and concentration distribution of benzene, CH<sub>4</sub>, and O<sub>2</sub>. This material is available free of charge via the Internet at <http://pubs.acs.org>.

## ■ AUTHOR INFORMATION

### Corresponding Author

\*Phone: 713-348-5903; fax: 713-348-5203; e-mail: [alvarez@rice.edu](mailto:alvarez@rice.edu).

### Notes

The authors declare no competing financial interest.

## ■ ACKNOWLEDGMENTS

This work was funded by the American Petroleum Institute. Jie Ma also received partial support from a scholarship from the China Scholarship Council. We thank Dr. Qiyu Jiang for his help with the shared computing facilities at Rice University.

## ■ REFERENCES

- (1) EPA. *Renewable Fuels: Regulations and Standards*; U.S. Environmental Protection Agency: Washington, DC, US, 2012.
- (2) Ma, J.; Rixey, W. G.; Alvarez, P. J. J. Microbial processes influencing the transport, fate and groundwater impacts of fuel ethanol releases. *Curr. Opin. Biotechnol.* **2013**, *24* (3), 457–466.
- (3) Ma, J.; Rixey, W. G.; DeVaul, G. E.; Stafford, B. P.; Alvarez, P. J. J. Methane bioattenuation and implications for explosion risk reduction along the groundwater to soil surface pathway above a plume of dissolved ethanol. *Environ. Sci. Technol.* **2012**, *46* (11), 6013–6019.
- (4) Sihota, N. J.; Mayer, K. U.; Toso, M. A.; Atwater, J. F. Methane emissions and contaminant degradation rates at sites affected by accidental releases of denatured fuel-grade ethanol. *J. Contam. Hydrol.* **2013**, *151* (0), 1–15.
- (5) Wilson, J. T.; Toso, M.; Mackay, D.; Sieyes, N. d.; DeVaul, G. E. *What's the Deal with Methane at LUST Spill Sites? Part 1*; New England Interstate Water Pollution Control Commission: Lowell, MA, US, 2012; Vol. 71: 6–8 and 13.
- (6) Jewell, K. P.; Wilson, J. T. A new screening method for methane in soil gas using existing groundwater monitoring wells. *Ground Water Monit. Remediat.* **2011**, *31* (3), 82–94.
- (7) Nelson, D. K.; Lapara, T. M.; Novak, P. J. Effects of ethanol-based fuel contamination: Microbial community changes, production of regulated compounds, and methane generation. *Environ. Sci. Technol.* **2010**, *44* (12), 4525–4530.
- (8) Freitas, J. G.; Fletcher, B.; Aravena, R.; Barker, J. F. Methane production and isotopic fingerprinting in ethanol fuel contaminated sites. *Ground Water* **2010**, *48* (6), 844–857.
- (9) Jourabchi, P.; Hers, I.; Mayer, K. U.; Devaul, G. E.; Kolhatkar, R. V. Numerical Modeling Study of the Influence of Methane Generation from Ethanol-Gasoline Blends on Vapor Intrusion. In *The Second*

*International Symposium on Bioremediation and Sustainable Environmental Technologies*, Jacksonville, FL, US; 2013, Jacksonville, FL, US.

(10) Wilson, J. T.; Toso, M.; Mackay, D.; Sieyes, N. d.; DeVaul, G. E. *What's the Deal with Methane at LUST Spill Sites? Part 2: Vapor Intrusion*; New England Interstate Water Pollution Control Commission: Lowell, MA, US, 2013; Vol. 72: pp 5–11 and 21–22.

(11) Spalding, R. F.; Toso, M. A.; Exner, M. E.; Hattan, G.; Higgins, T. M.; Sekely, A. C.; Jensen, S. D. Long-term groundwater monitoring results at large, sudden denatured ethanol releases. *Ground Water Monit. Remediat.* **2011**, *31* (3), 69–81.

(12) Ma, J.; Xiu, Z.; Monier, A.; Mamonkina, I.; Zhang, Y.; He, Y.; Stafford, B.; Rixey, W.; Alvarez, P. Aesthetic groundwater quality Impacts from a continuous pilot-scale release of an ethanol blend. *Ground Water Monit. Remediat.* **2011**, *31* (3), 47–54.

(13) Patterson, B. M.; Davis, G. B. Quantification of vapor intrusion pathways into a slab-on-ground building under varying environmental conditions. *Environ. Sci. Technol.* **2009**, *43* (3), 650–656.

(14) Baird, A. J.; Beckwith, C. W.; Waldron, S.; Waddington, J. M. Ebullition of methane-containing gas bubbles from near-surface Sphagnum peat. *Geophys. Res. Lett.* **2004**, *31*, (21).

(15) Jain, N.; Pathak, H.; Mitra, S.; Bhatia, A. Emission of methane from rice fields—A review. *J. Sci. Ind. Res.* **2004**, *63* (2), 101–115.

(16) Amos, R. T.; Mayer, K. U. Investigating ebullition in a sand column using dissolved gas analysis and reactive transport modeling. *Environ. Sci. Technol.* **2006**, *40* (17), 5361–5367.

(17) Molins, S.; Mayer, K. U.; Scheutz, C.; Kjeldsen, P. Transport and reaction processes affecting the attenuation of landfill gas in cover soils. *J. Environ. Qual.* **2008**, *37* (2), 459–468.

(18) Molins, S.; Mayer, K. U.; Amos, R. T.; Bekins, B. A. Vadose zone attenuation of organic compounds at a crude oil spill site—Interactions between biogeochemical reactions and multicomponent gas transport. *J. Contam. Hydrol.* **2010**, *112* (1–4), 15–29.

(19) Amos, R. T.; Mayer, K. U.; Bekins, B. A.; Delin, G. N.; Williams, R. L. Use of dissolved and vapor-phase gases to investigate methanogenic degradation of petroleum hydrocarbon contamination in the subsurface. *Water Resour. Res.* **2005**, *41*, (2).

(20) Lundegard, P. D.; Johnson, P. C.; Dahlen, P. Oxygen transport from the atmosphere to soil gas beneath a slab-on-grade foundation overlying petroleum-impacted soil. *Environ. Sci. Technol.* **2008**, *42* (15), 5534–5540.

(21) Hers, I.; Atwater, J.; Li, L.; Zapf-Gilje, R. Evaluation of vadose zone biodegradation of BTX vapours. *J. Contam. Hydrol.* **2000**, *46* (3–4), 233–264.

(22) Fitzpatrick, N. A.; Fitzgerald, J. J. An evaluation of vapor intrusion into buildings through a study of field data. *Soil Sediment Contam.* **2002**, *11* (4), 603–623.

(23) Johnson, P. C.; Ettinger, R. A. Heuristic model for predicting the intrusion rate of contaminant vapors into buildings. *Environ. Sci. Technol.* **1991**, *25* (8), 1445–1452.

(24) DeVaul, G. E. Indoor vapor intrusion with oxygen-limited biodegradation for a subsurface gasoline source. *Environ. Sci. Technol.* **2007**, *41* (9), 3241–3248.

(25) Abreu, L. D. V.; Johnson, P. C. Effect of vapor source—Building separation and building construction on soil vapor intrusion as studied with a three-dimensional numerical model. *Environ. Sci. Technol.* **2005**, *39* (12), 4550–4561.

(26) Johnson, P. C.; Kembroski, M. W.; Johnson, R. L. Assessing the significance of subsurface contaminant vapor migration to enclosed spaces: Site-specific alternatives to generic estimates. *J. Soil Contam.* **1999**, *8* (3), 389–421.

(27) Mills, W. B.; Liu, S.; Rigby, M. C.; Brenner, D. Time-variable simulation of soil vapor intrusion into a building with a combined crawl space and basement. *Environ. Sci. Technol.* **2007**, *41* (14), 4993–5001.

(28) Pennell, K. G.; Bozkurt, O.; Suuberg, E. M. Development and application of a three-dimensional finite element vapor intrusion model. *J. Air Waste Manage. Assoc.* **2009**, *59* (4), 447–460.

- (29) Yu, S.; Unger, A. J. A.; Parker, B. Simulating the fate and transport of TCE from groundwater to indoor air. *J. Contam. Hydrol.* **2009**, *107* (3–4), 140–161.
- (30) Parker, J. C. Modeling volatile chemical transport, biodecay, and emission to indoor air. *Ground Water Monit. Remediat.* **2003**, *23* (1), 107–120.
- (31) Verginelli, I.; Baciocchi, R. Modeling of vapor intrusion from hydrocarbon-contaminated sources accounting for aerobic and anaerobic biodegradation. *J. Contam. Hydrol.* **2011**, *126* (3–4), 167–180.
- (32) Abreu, L. D. V.; Ettinger, R.; McAlary, T. Simulated soil vapor intrusion attenuation factors including biodegradation for petroleum hydrocarbons. *Ground Water Monit. Remediat.* **2009**, *29* (1), 105–117.
- (33) Abreu, L. D. V.; Johnson, P. C. Simulating the effect of aerobic biodegradation on soil vapor intrusion into buildings: Influence of degradation rate, source concentration, and depth. *Environ. Sci. Technol.* **2006**, *40* (7), 2304–2315.
- (34) Bozkurt, O.; Pennell, K. G.; Suuberg, E. M. Simulation of the vapor intrusion process for nonhomogeneous soils using a three-dimensional numerical model. *Ground Water Monit. Remediat.* **2009**, *29* (1), 92–104.
- (35) Yao, Y. J.; Shen, R.; Pennell, K. G.; Suuberg, E. M. Comparison of the Johnson-Ettinger vapor intrusion screening model predictions with full three-dimensional model results. *Environ. Sci. Technol.* **2011**, *45* (6), 2227–2235.
- (36) Abreu, L. D. V. A transient three-dimensional numerical model to simulate vapor intrusion into building. Ph.D. Dissertation; Arizona State University: Tempe, AZ, 2005.
- (37) EPA. *EPA's Vapor Intrusion Database: Evaluation and Characterization of Attenuation Factors for Chlorinated Volatile Organic Compounds and Residential Buildings*; Office of Solid Waste and Emergency Response, U.S. Environmental Protection Agency: Washington, DC, 2012.
- (38) EPA. *Conceptual Model Scenarios for the Vapor Intrusion Pathway*; Office of Solid Waste and Emergency Response, U.S. Environmental Protection Agency: Washington, DC, 2012.
- (39) EPA. *Evaluation Of Empirical Data To Support Soil Vapor Intrusion Screening Criteria For Petroleum Hydrocarbon Compounds*; Office of Underground Storage Tanks, U.S. Environmental Protection Agency: Washington, DC, 2013.
- (40) Lahvis, M. A.; Hers, I.; Davis, R. V.; Wright, J.; DeVaul, G. E. Vapor intrusion screening at petroleum UST sites. *Groundwater Monit. Remediat.* **2013**, *33* (2), 53–67.
- (41) Nastev, M.; Therrien, R.; Lefebvre, R.; Gelinas, P. Gas production and migration in landfills and geological materials. *J. Contam. Hydrol.* **2001**, *52* (1–4), 187–211.
- (42) Robinson, A. L.; Sextro, R. G. Radon entry into buildings driven by atmospheric pressure fluctuations. *Environ. Sci. Technol.* **1997**, *31* (6), 1742–1748.
- (43) Riley, W. J.; Robinson, A. L.; Gadgil, A. J.; Nazaroff, W. W. Effects of variable wind speed and direction on radon transport from soil into buildings: model development and exploratory results. *Atmos. Environ.* **1999**, *33* (14), 2157–2168.
- (44) Luo, H. Field and modeling studies of soil vapor migration into buildings at petroleum hydrocarbon impacted sites. Ph.D. Dissertation, Arizona State University: Phoenix, AZ, US, 2009.
- (45) Cunningham, R. E.; Williams, R. J. *Diffusion in Gases and Porous Media*; Plenum Press: New York, NY, US, 1980.
- (46) Mason, E. A.; Malinauskas, A. P. *Gas Transport in Porous Media: The Dusty-Gas Model (Chemical Engineering Monographs)*; Elsevier Science Ltd: New York, NY, US, 1983.
- (47) Hanson, R. S.; Hanson, T. E. Methanotrophic bacteria. *Microbiol. Rev.* **1996**, *60* (2), 439–471.
- (48) EPA. *OSWER Draft Guidance for Evaluating the Vapor Intrusion to Indoor Air Pathway from Groundwater and Soils (Subsurface Vapor Intrusion Guidance)*; U.S. Environmental Protection Agency: Washington, DC, 2002.
- (49) Vogt, C.; Kleinstuber, S.; Richnow, H. H. Anaerobic benzene degradation by bacteria. *Microbial Biotechnol.* **2011**, *4* (6), 710–724.
- (50) Singh, S.; Singh, J. S.; Kashyap, A. K. Methane flux from irrigated rice fields in relation to crop growth and N-fertilization. *Soil Biol. Biochem.* **1999**, *31* (9), 1219–1228.
- (51) Datta, A.; Yeluripati, J. B.; Nayak, D. R.; Mahata, K. R.; Santra, S. C.; Adhya, T. K. Seasonal variation of methane flux from coastal saline rice field with the application of different organic manures. *Atmos. Environ.* **2013**, *66*, 114–122.
- (52) Elberling, B.; Askaer, L.; Jorgensen, C. J.; Joensen, H. P.; Kuhl, M.; Glud, R. N.; Lauritsen, F. R. Linking soil O<sub>2</sub>, CO<sub>2</sub>, and CH<sub>4</sub> concentrations in a wetland soil: Implications for CO<sub>2</sub> and CH<sub>4</sub> fluxes. *Environ. Sci. Technol.* **2011**, *45* (8), 3393–3399.
- (53) Alford, D. P.; Delaune, R. D.; Lindau, C. W. Methane flux from Mississippi River deltaic plain wetlands. *Biogeochemistry* **1997**, *37* (3), 227–236.
- (54) Hirota, M.; Senga, Y.; Seike, Y.; Nohara, S.; Kunii, H. Fluxes of carbon dioxide, methane and nitrous oxide in two contrastive fringing zones of coastal lagoon, Lake Nakaumi, Japan. *Chemosphere* **2007**, *68* (3), 597–603.
- (55) Deborde, J.; Anschutz, P.; Guerin, F.; Poirier, D.; Marty, D.; Boucher, G.; Thouzeau, G.; Canton, M.; Abril, G. Methane sources, sinks and fluxes in a temperate tidal Lagoon: The Arcachon lagoon (SW France). *Estuar. Coastal Shelf Sci.* **2010**, *89* (4), 256–266.
- (56) Bohdalkova, L.; Curik, J.; Kubena, A. A.; Buzek, F. Dynamics of methane fluxes from two peat bogs in the Ore Mountains, Czech Republic. *Plant Soil Environ.* **2013**, *59* (1), 14–21.
- (57) Smemo, K. A.; Yavitt, J. B. A multi-year perspective on methane cycling in a shallow peat fen in central New York State, USA. *Wetlands* **2006**, *26* (1), 20–29.
- (58) Bogner, J.; Meadows, M.; Czepiel, P. Fluxes of methane between landfills and the atmosphere: Natural and engineered controls. *Soil Use Manage.* **1997**, *13* (4), 268–277.
- (59) Cardellini, C.; Chioldini, G.; Frondini, F.; Granieri, D.; Lewicki, J.; Peruzzi, L. Accumulation chamber measurements of methane fluxes: Application to volcanic-geothermal areas and landfills. *Appl. Geochem.* **2003**, *18* (1), 45–54.